Supporting Information

Fluorinated ether based electrolyte enabling sodium-metal batteries with exceptional cycling stability

Qiang Yi,[1,2] Yao Lu[1], Xiaorui Sun[2,3], Hua Zhang[3], Hailong Yu[3] and Chunwen Sun[1,2*]

[1]CAS Center for Excellence in Nanoscience, Beijing Institute of Nanoenergy and Nanosystems, Chinese Academy of Sciences, Beijing 100083, P. R. China

[2]School of Nanoscience and Technology, University of Chinese Academy of Sciences, Beijing 100049, P. R. China

[3]Beijing National Laboratory for Condensed Matter Physics, Institute of Physics, Chinese Academy of Sciences, Beijing 100190, P. R. China

[*] Corresponding authors.

Tel.: +86-10-82854648, fax: +86-10-82854648. Email: sunchunwen@binn.cas.cn (C. Sun)

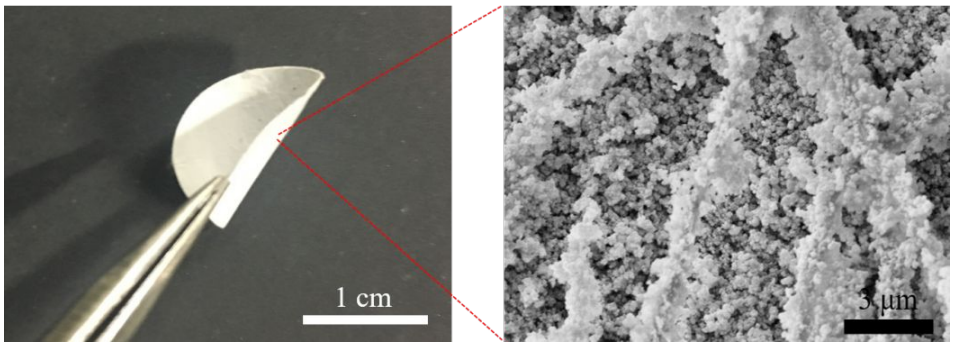

Figure S1. Photographs and SEM images of the nonflammable porous separator (NPS).

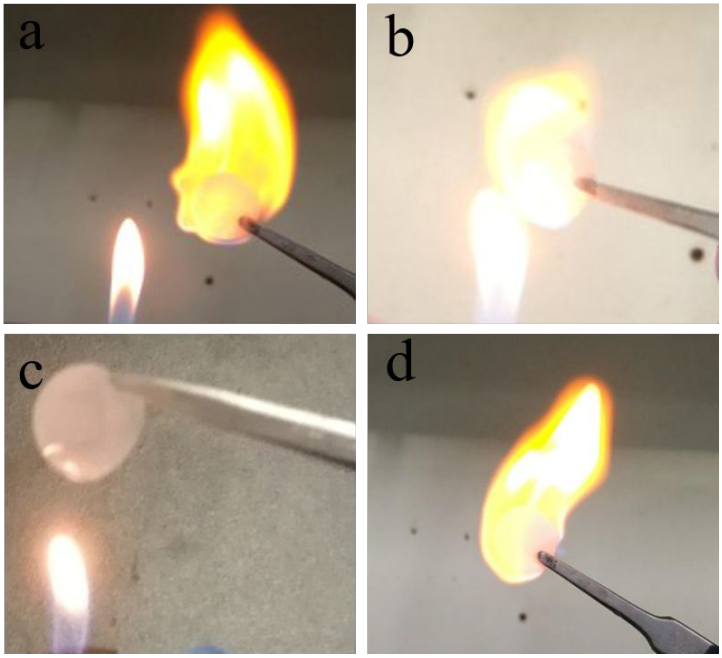

Figure S2. Flame test of different electrolytes absorbed in porous separators: (a) $NaPF_6$-DME, (b) $NaPF_6$-FE and (c) $NaPF_6$-FRE, (d) EC/PC based liquid electrolyte.

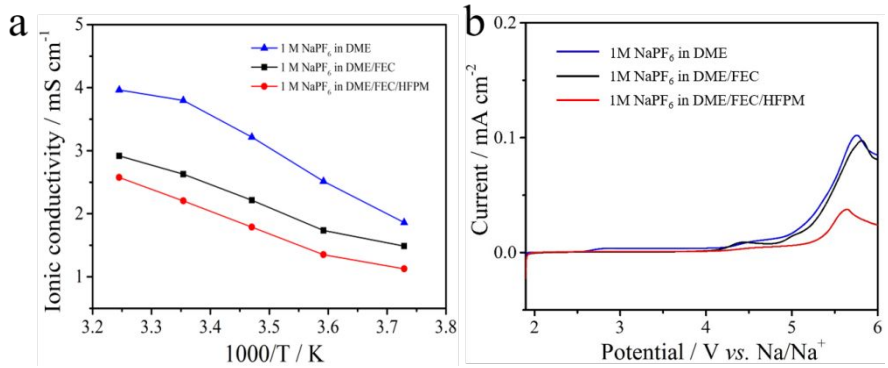

Figure S3. (a) Ionic conductivities of different electrolytes at different temperatures. (b) The electrochemical window of different electrolytes evaluated by a linear sweep voltammetry (LSV) from 1.9 V to 6.0 V.

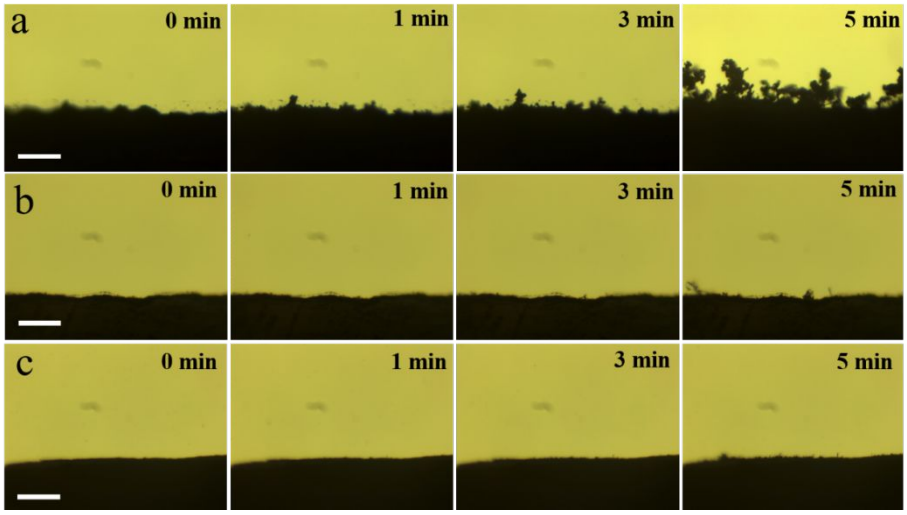

Figure S4. In situ optical observations of Na plating in different electrolytes: (a) $NaPF_6$-DME, (b) $NaPF_6$-FE and (c) $NaPF_6$-FRE. All the scale bars are 500 μm. The plating current is 2 mA cm^{-2}.

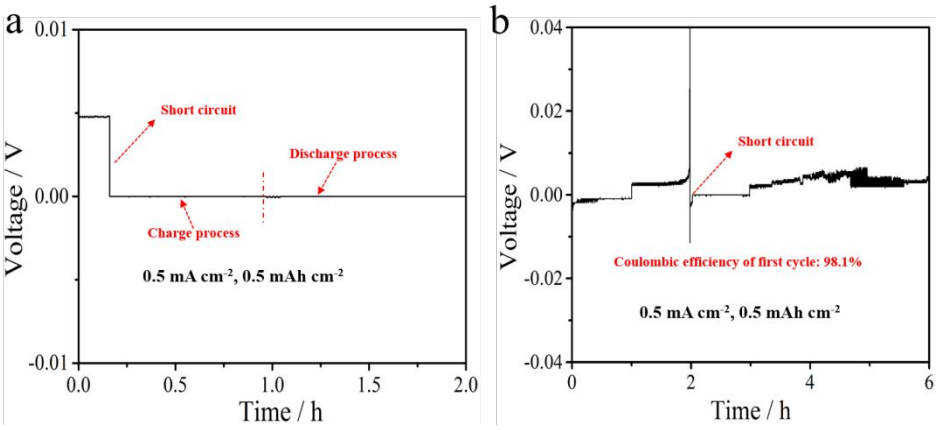

Figure S5. (a) Cycling performance of the Na symmetric cell with $NaPF_6$-DME electrolyte at 0.5 mA cm^{-2} and 0.5 mAh cm^{-2}. (b) Cycling performance of the Na ||Cu cell with $NaPF_6$-DME electrolyte at 0.5 mA cm^{-2} and 0.5 mAh cm^{-2}.

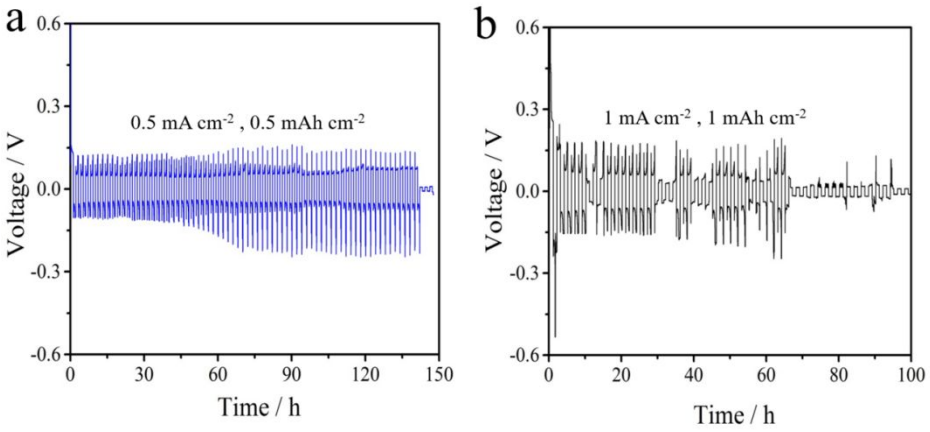

Figure S6. Cycling performance of Na symmetric cells with commercial carbonate-based electrolyte: (a) at 0.5 mA cm^{-2} and 0.5 mAh cm^{-2}, and (b) at 1 mA cm^{-2} and 1 mAh cm^{-2}.

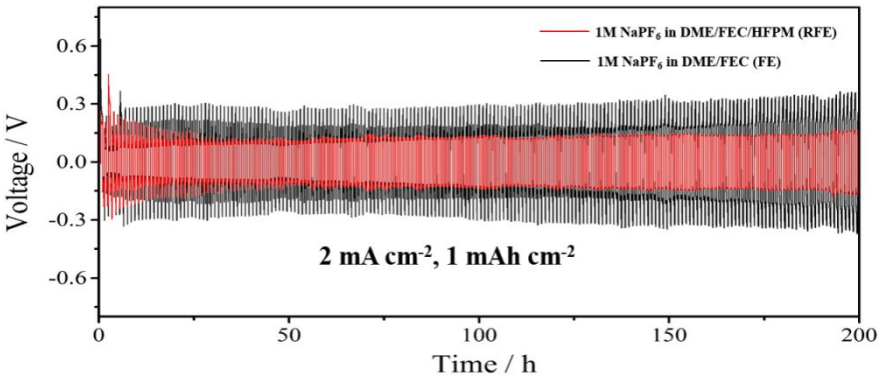

Figure S7. Cycling performance of the Na symmetric cell with $NaPF_6$-FRE electrolyte absorbed in NPS at 2 mA cm^{-2} and 1 mAh cm^{-2}.

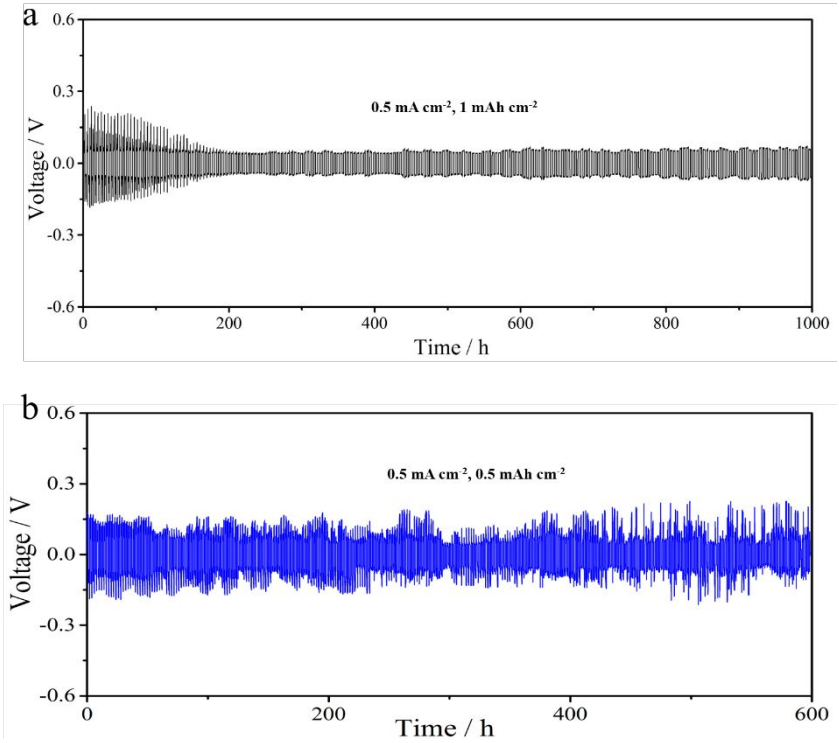

Figure S8. Cycling performance of the Na symmetric cell with (a) $NaPF_6$-FRE electrolyte absorbed in glass fiber separator at 0.5 mA cm^{-2} and 1 mAh cm^{-2} and (b) $NaPF_6$-FE electrolyte absorbed in glass fiber separator at 0.5 mA cm^{-2} and 0.5 mAh cm^{-2}.

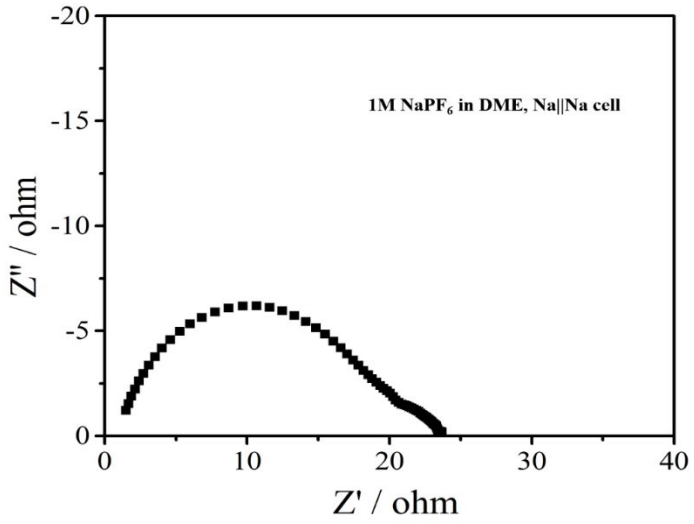

Figure S9. Nyquist plots of the Na symmetric cell with $NaPF_6$-DME electrolyte before cycling test.

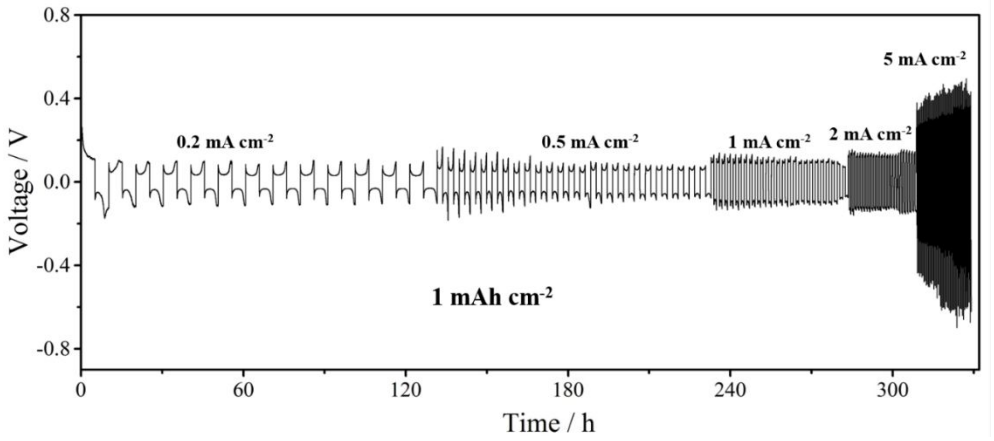

Figure S10. Rate performance of the Na symmetric cells with $NaPF_6$-FRE electrolyte absorbed in NPS at different current densities.

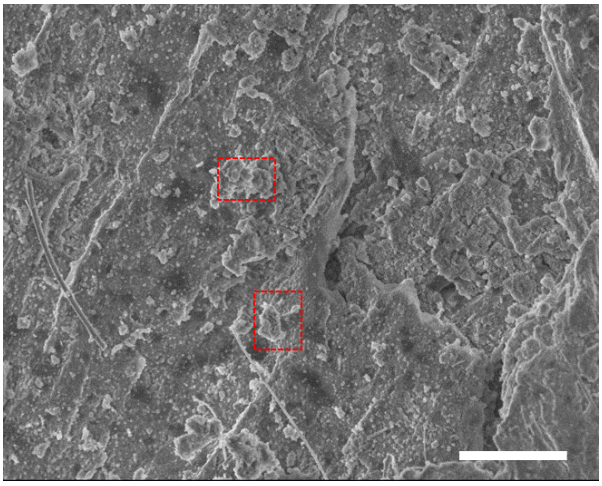

Figure S11. SEM images of the Na surface in the cell with Commercial $NaPF_6$-EC/PC electrolyte after 2 cycles at 0.5 mA cm^{-2} and 1mAh cm^{-2}. The scale bars are 5 μm.

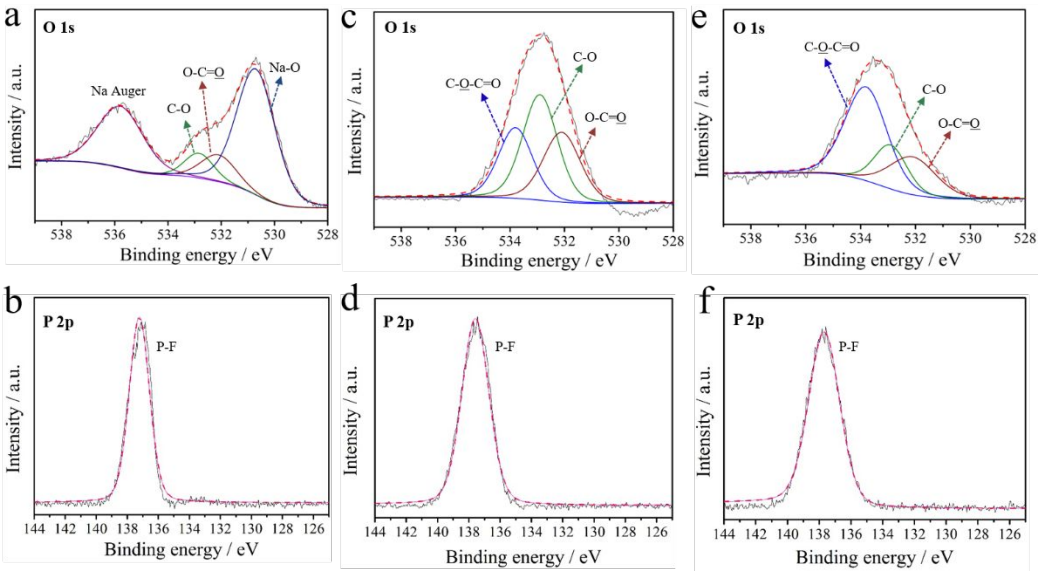

Figure S12. XPS spectra of Na surface after 50 cycles at 1 mA cm^{-2} with different electrolytes: O1s and P2p spectra of Na surface after cycling with $NaPF_6$-DME (a, b), $NaPF_6$-FE (c, d) and $NaPF_6$-FRE and (e, f) electrolyte.

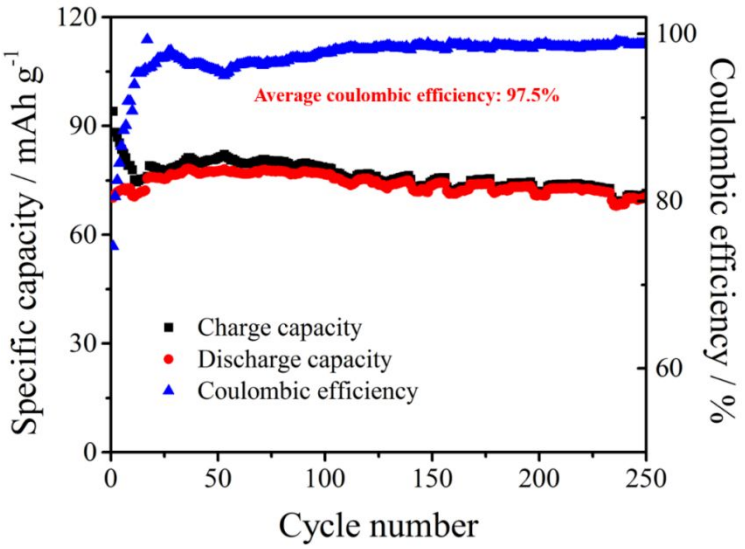

Figure S13. Cycling performance of the NVP||Na cells with 1M $NaPF_6$-DME electrolyte absorbed in glass fiber at 0.5 C.

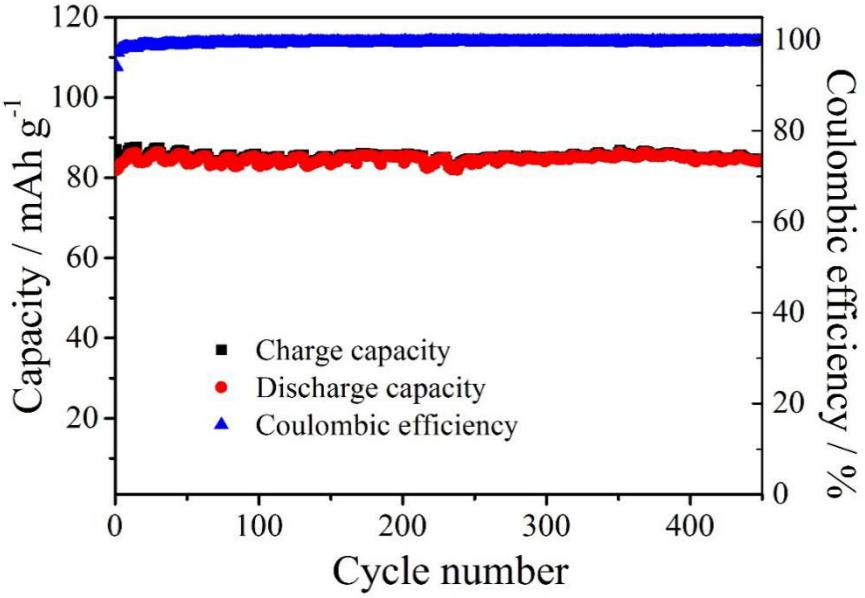

Figure S14. Cycling performance of the NVP||Na cells with 1M $NaPF_6$-FE electrolyte absorbed in NPS at 0.5 C.

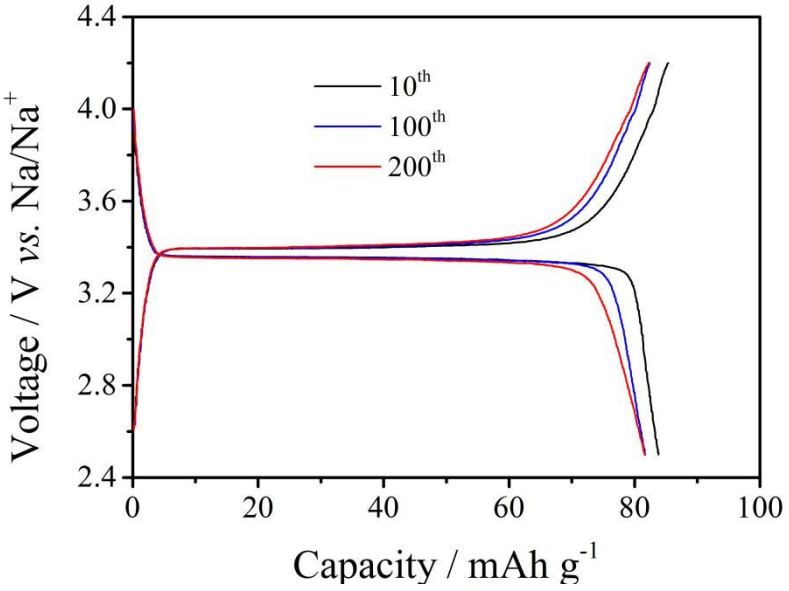

Figure S15. Typical charge/discharge curves of the NVP||Na cell with 1M $NaPF_6$-DME electrolyte absorbed in NPS at 0.5 C after different cycles.

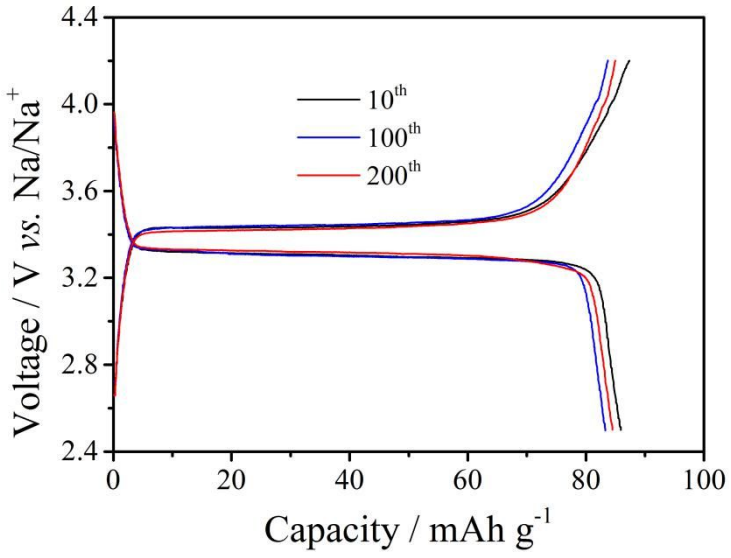

Figure S16. Typical charge/discharge curves of the NVP||Na cell with 1M $NaPF_6$-FE electrolyte absorbed in NPS at 0.5 C after different cycles.

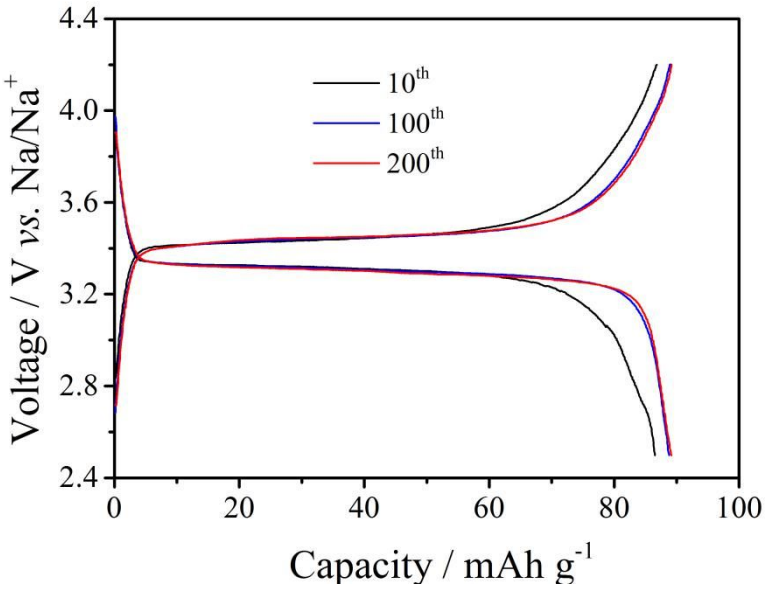

Figure S17. Typical charge/discharge curves of the NVP||Na cell with 1M $NaPF_6$-FRE electrolyte absorbed in NPS at 0.5 C after different cycles.

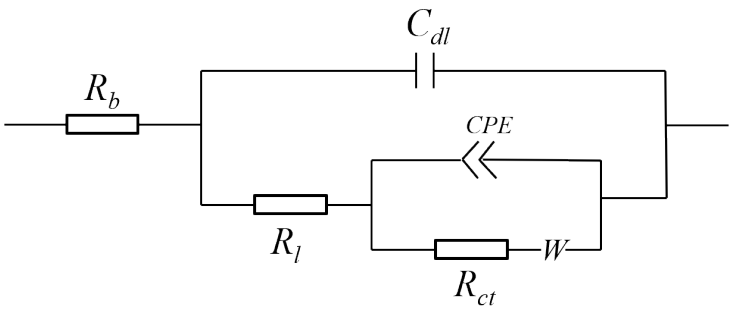

Figure S18. Equivalent circuit utilized for fitting electrochemical impedance spectroscopy. R_b, R_l, R_{ct} and Z_w corresponding to bulk resistance, liquid electrolyte resistance, charge transfer resistance and Warburg impedance.[S1-S2] Interfacial resistance (R_i) corresponds to the intercept of the semi-circle with the real axis at the lower frequency.

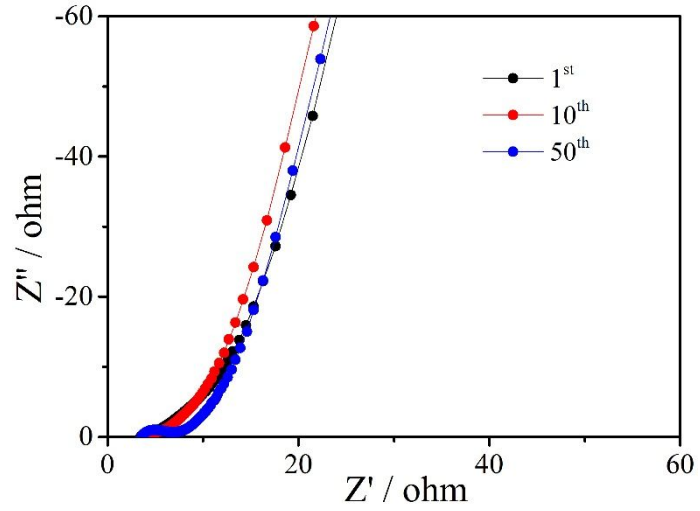

Figure S19. Nyquist plots of the NVP||Na cell with $NaPF_6$-DME electrolyte after different cycles at 1 C.

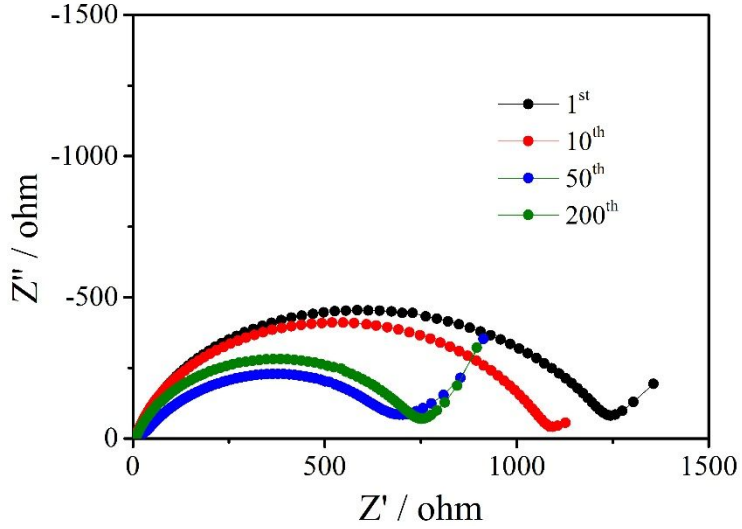

Figure S20. Nyquist plots of the NVP||Na cell with $NaPF_6$-FE electrolyte after different cycles at 1 C.

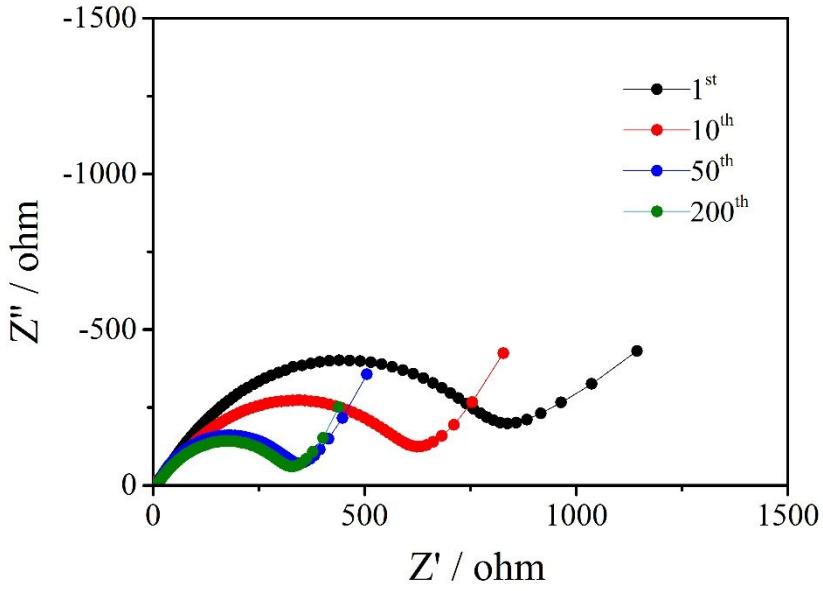

Figure S21. Nyquist plots of NVP||Na cell with $NaPF_6$-FRE electrolyte after different cycles at 1 C.

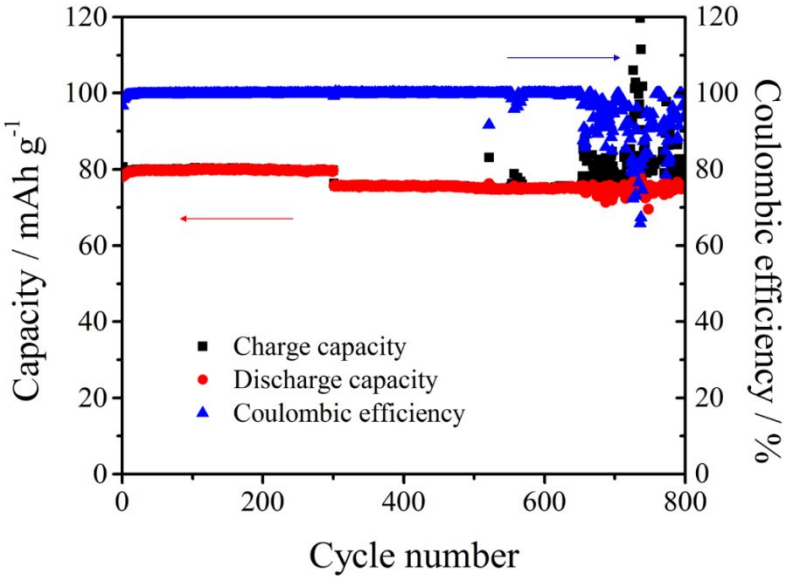

Figure S22. Cycling performance of the NVP||Na cells with commercial carbonate-based electrolyte absorbed in NPS at 0.5 C and 1C.

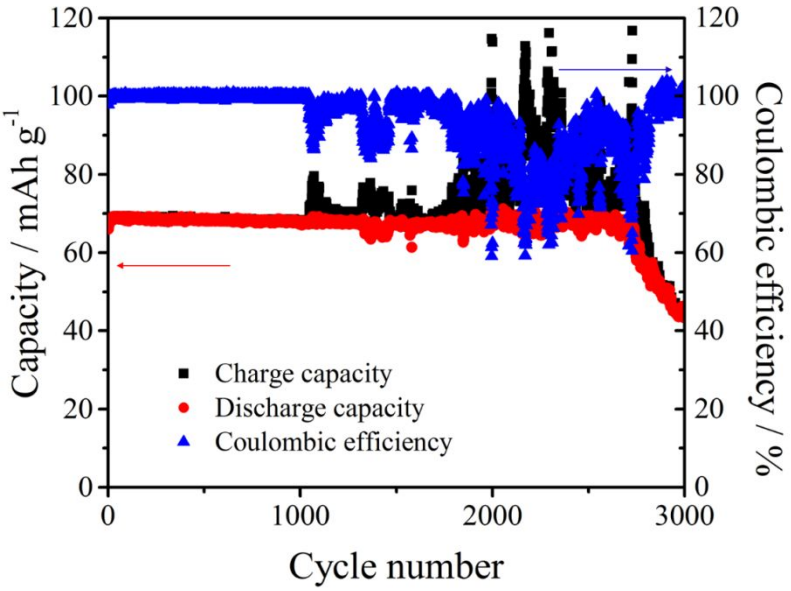

Figure S23. Cycling performance of the NVP||Na cells with commercial carbonate-based electrolyte absorbed in NPS at 5 C.

Table S1. Comparison of the cycling performance of NVP-based cathodes based cells with different electrolytes cycled at 5 C.

Cathode	Electrolyte	Capacity retention	Reference
NVP@rGO	1M $NaClO_4$ in EC/DMC	81% after 3000 cycles	S3
NVP@C	1M $NaClO_4$ in PC	88% after 700 cycles	S4
NVP@C@CMK-3	1M $NaClO_4$ in PC/FEC	68% after 2000 cycles	S5
NVP@C@HC	1M $NaClO_4$ in EC/DMC/FEC	90.4% after 500 cycles	S6
NVP	1M $NaPF_4$ in DME/FEC/HFPM	94.1% after 2000 cycles	This work

References

(S1) Ates, M.; Sarac, A. S. Capacitive Behavior of Polycarbazole and Poly (N-vinylcarbazole)-Coated Carbon Fiber Microelectrodes in Various Solutions. *J.*

Appl. Electrochem. **2009**, *39*, 2043−2048.

(S2) Sarac, A. S.; Ates, M.; Kilic, B. Electrochemical Impedance Spectroscopic Study of Polyaniline on Platinum, Glassy Carbon and 661 Carbon Fiber Microelectrodes. *Int. J. Electrochem. Sci.* **2008**, *3*, 777− 662786.

(S3) Zhang, J.; Fang, Y.; Xiao, L.; Qian, J.; Cao,Y.; Ai, X.;Yang, H. Graphene-Scaffolded Na_3V_2 $(PO_4)_3$ Microsphere Cathode with High Rate Capability and Cycling Stability for Sodium Ion Batteries. *ACS Appl. Mater. Interfaces* **2017**, *9*, 7177−7184.

(S4) Shen, W.; Li, H.; Guo, Z.; Wang, C.; Li, Z.; Xu, Q.; Liu, H.; Wang, Y.; Xia, Y. Double-Nanocarbon Synergistically Modified $Na_3V_2(PO_4)_3$: an Advanced Cathode for High-Rate and Long-Life Sodium-Ion Batteries. *ACS Appl. Mater. Interfaces* **2016**, *8*, 15341-15351.

(S5) Jiang, Y.; Yang, Z.; Li, W.; Zeng, L.; Pan, z.; Wang, M.; Wei, X.; Hu, G.; Gu, L.; Yu, Y. Nanoconfined Carbon-Coated $Na_3V_2(PO_4)_3$ Particles in Mesoporous Carbon Enabling Ultralong Cycle Life for Sodium-Ion Batteries. *Adv. Energy Mater.* **2015**, *5*, 1402104.

(S6) Chen, L.; Zhao, Y.; Liu, S.; Zhao, L. Hard Carbon Wrapped $Na_3V_2(PO_4)_3$@C Porous Composite Extending Cycling Lifespan for Sodium-Ion Batteries. *ACS Appl. Mater. Interfaces* **2017**, *9*, 44485-44493.